

Design and Evaluation of a Compliant Quasi Direct Drive End-effector for Safe Robotic Ultrasound Imaging

Danyi Chen^{*1}, Ravi Prakash¹, Zacharias Chen¹, Sarah Dias², Vincent Wang¹,
Leila Bridgeman¹, and Siobhan Oca¹

¹Thomas Lord Department of Mechanical Engineering and Materials Science, Duke University, NC, USA

²Research Triangle High School, NC, USA

Abstract—Robot-assisted ultrasound scanning promises to advance autonomous and accessible medical imaging. However, ensuring patient safety and compliant human-robot interaction (HRI) during probe contact poses a significant challenge. Most existing systems either have high mechanical stiffness or are compliant but lack sufficient force and precision. This paper presents a novel single-degree-of-freedom end-effector for safe and accurate robotic ultrasound imaging, using a quasi-direct drive actuator to achieve both passive mechanical compliance and precise active force regulation, even during motion. The end-effector demonstrates an effective force control bandwidth of 100 Hz and can apply forces ranging from 2.5N to 15N. To validate the end-effector’s performance, we developed a novel *ex vivo* actuating platform, enabling compliance testing of the end-effector on simulated abdominal breathing and sudden patient movements. Experiments demonstrate that the end-effector can maintain consistent probe contact during simulated respiratory motion at 2.5N, 5N, 10N, and 15N, with an average force tracking RMS error of 0.83N compared to 4.70N on a UR3e robot arm using conventional force control. This system represents the first compliant ultrasound end-effector tested on a tissue platform simulating dynamic movement. The proposed solution provides a novel approach for designing and evaluating compliant robotic ultrasound systems, advancing the path for more compliant and patient-friendly robotic ultrasound systems in clinical settings.

I. INTRODUCTION

Ultrasound (US) imaging has been a reliable and versatile diagnostic tool since the mid-20th century, widely used due to its non-invasive nature, real-time imaging, lack of ionizing radiation, and relatively low cost [1]. However, conventional US exams rely heavily on trained sonographers to apply consistent pressure and precisely control the probe’s orientation, impacting the consistency and accuracy of diagnostic results. The increasing demand for US exams has outpaced the growth in the number of sonographers, particularly affecting remote or underserved areas [2] [3]. Robotic US systems offer significant advantages, automating probe manipulation to reduce physical stress on sonographers and improve imaging precision and reproducibility [4]. These systems can also operate autonomously, enabling US imaging in high-latency environments like space missions or remote

This work is supported in part by the National Science Foundation Traineeship in the Advancement of Surgical Technologies (TAST) program, the Innovation Co-Lab at Duke University’s Office of Information Technology, and the Thomas Lord Department of Mechanical Engineering and Materials Science.

*Corresponding author: Danyi Chen (dc442@duke.edu)

locations, extending access to diagnostics in areas with limited healthcare professionals [4].

Despite their advantages, the integration of robotic US systems into clinical practice faces significant challenges, particularly concerning patient safety and human-robot interaction (HRI). A major concern is the potential for excessive force exerted by the robot end-effector, typically rigid and non-mechanically compliant, which can lead to patient discomfort or even injury [5] [6]. Ensuring compliance - the system’s ability to adapt and yield under applied force without causing excessive pressure, in the contact between the probe and the patient’s body is essential to mitigate this risk. This is especially critical for abdominal imaging, where movements of the abdominal wall during respiration would require a robotic system to adapt dynamically to maintain consistent and safe contact with the skin [7]. While sonographers typically instruct the patient to hold their breath, breathing will still occur since scanning sessions can last up to 30 minutes. In addition, robots will also have to handle unexpected movements from the patient during scans.

Researchers have explored active and passive compliance methods to address compliance challenges [8]. Active compliance enables a rigid robot arm to exhibit compliant behavior by controlling the end-effector position based on force or torque input, often using task-space force controllers with admittance and impedance strategies to simulate spring-damper behaviors [9] [10]. However, these methods are limited by low bandwidths, making them slow to respond to sudden movements [11]. Passive compliance, achieved by integrating mechanically compliant elements, allows the robot to physically deflect or deform in response to external forces without a controller. This includes soft materials, fluidic actuators, and compliant pneumatic actuators [5], [12]. However, soft end-effectors apply variable force based on deformation, and while pneumatic actuators can regulate force, they are noisy and nonlinear, limiting their bandwidth [13] [14]. Neither approach has achieved more than 10N of contact force, falling short of clinical requirements, nor included position feedback, which is critical for effective scanning algorithms.

While electric motors offer improved bandwidth and ease of control in comparison to pneumatic and fluidic actuators, traditional electric motors used in robotic arms often lack mechanical compliance due to their high gear ratios and

significant backdrive force [15]. However, recent advancements have led to the development of quasi-direct drive (QDD) actuators, which could achieve high torque and high bandwidths while having a low backdrive torque, allowing external forces to backdrive the motor and achieve compliance mechanically [16].

For evaluation, a robust human-behavior mimicking platform is needed to facilitate fair and realistic evaluation of compliant ultrasound actuators. While several approaches have been developed to ensure safe and effective force control during ultrasound procedures, the platform is static. To our knowledge, there is no moving tissue platform that can accurately replicate the dynamic behavior of both physiological and unexpected human motion during abdominal ultrasound exams. This limits the ability to fully evaluate the performance of compliant ultrasound systems in realistic scenarios.

This paper proposes a novel single-degree-of-freedom end-effector for safe robotic US imaging. Our design uses QDD actuators to achieve several key advantages: passive mechanical compliance ensures safe patient interaction even in the event of control failure; precise active contact force control optimizes scanning quality; the high bandwidth response of QDD actuators enables fast real-time adjustments to dynamic movements; and the design has accurate feedback of the probe's position in space. To evaluate this end-effector, we propose a novel actuated *ex vivo* tissue platform to simulate the motion of the human abdomen during breathing and sudden unexpected movements.

II. METHODS

A. Clinically Informed Design Requirements

TABLE I: Clinically informed design requirements

	Clinical Requirement [17]	Active Compliance (Mathiassen16 [9])	Soft End-effector (Lindenroth17 [12])	Pneumatic Actuation (Kuo23 [5])	Our Proposed System
Range of Force	0N - 17.3N	1N - 5N	0N - 10N	4.1N - 7.5N	2.5N - 15N
Feedback	N/A	Position, Force	None	Force	Position, Force
Force Control Bandwidth	N/A	16.6hz	N/R	N/R	100hz
Active Force Regulation	N/A	Yes	No	Yes	Yes
Mechanical Compliance	N/A	No	Yes	Yes	Yes

Clinical US imaging requirements inform our design specifications, as seen in Table I. Our design focuses on key metrics such as applied force range, force control bandwidth, probe position feedback, and mechanical compliance, which are often inadequately addressed by existing solutions. This is particularly evident in force capability. For normal weight patients (BMI = 18.5–25), sonographers report typical contact forces during abdominal ultrasound scans ranging from

7.5 N (mean) to 17.3 N (max) [17]. Most state-of-the-art compliant US end-effectors fall short of reaching these force levels.

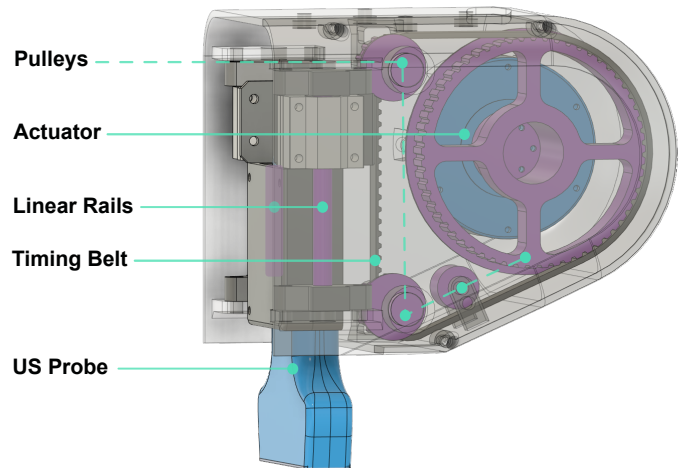


Fig. 1: CAD model of the compliant robotic US end-effector

B. Compliance Focused Actuation and Transmission Design

To achieve both passive compliance and high-bandwidth active force control, we opted for a mechanically compliant electric actuator. QDD actuators offer several advantages over pneumatic and soft fluidic actuators. First, they improve force control by eliminating the need for complex pressure regulation systems found in pneumatic actuators, which are often nonlinear and slower in response [13] [14]. The low gear ratio in QDD actuators allows for accurate force estimation based on output current and high bandwidths [18], leading to greater force control accuracy. Second, QDD actuators provide simplified control strategies, unlike soft fluidic actuators, which can exhibit unpredictable deformation and require more complex feedback systems to maintain force accuracy [19]. Lastly, unlike pneumatic and soft actuators, QDD actuators often have built-in positional feedback [20], requiring no extra sensor to determine the end-effector's position. QDD actuators have been successfully implemented in various fields requiring compliance, safe HRI, and impact absorption, including powered prostheses [21], powered orthoses [22], and legged robotics [11] [20]. For this study, we chose the AK60-6 (Cubemars, Shenzhen, China) QDD actuator, with a rated torque of 3Nm, a backdrive torque of 0.2Nm, and built-in positional feedback.

In order to convert rotational motion from the actuator into linear motion, a timing belt-driven transmission system was implemented. The inherent properties of the belt material provided intrinsic impact absorption, providing additional compliance in the system over more rigid methods such as gear transmissions. The timing belt system also has a simpler force transmission compared to alternative mechanisms such as crank-slider linkages, resulting in a more linear relationship between input rotation and output linear motion.

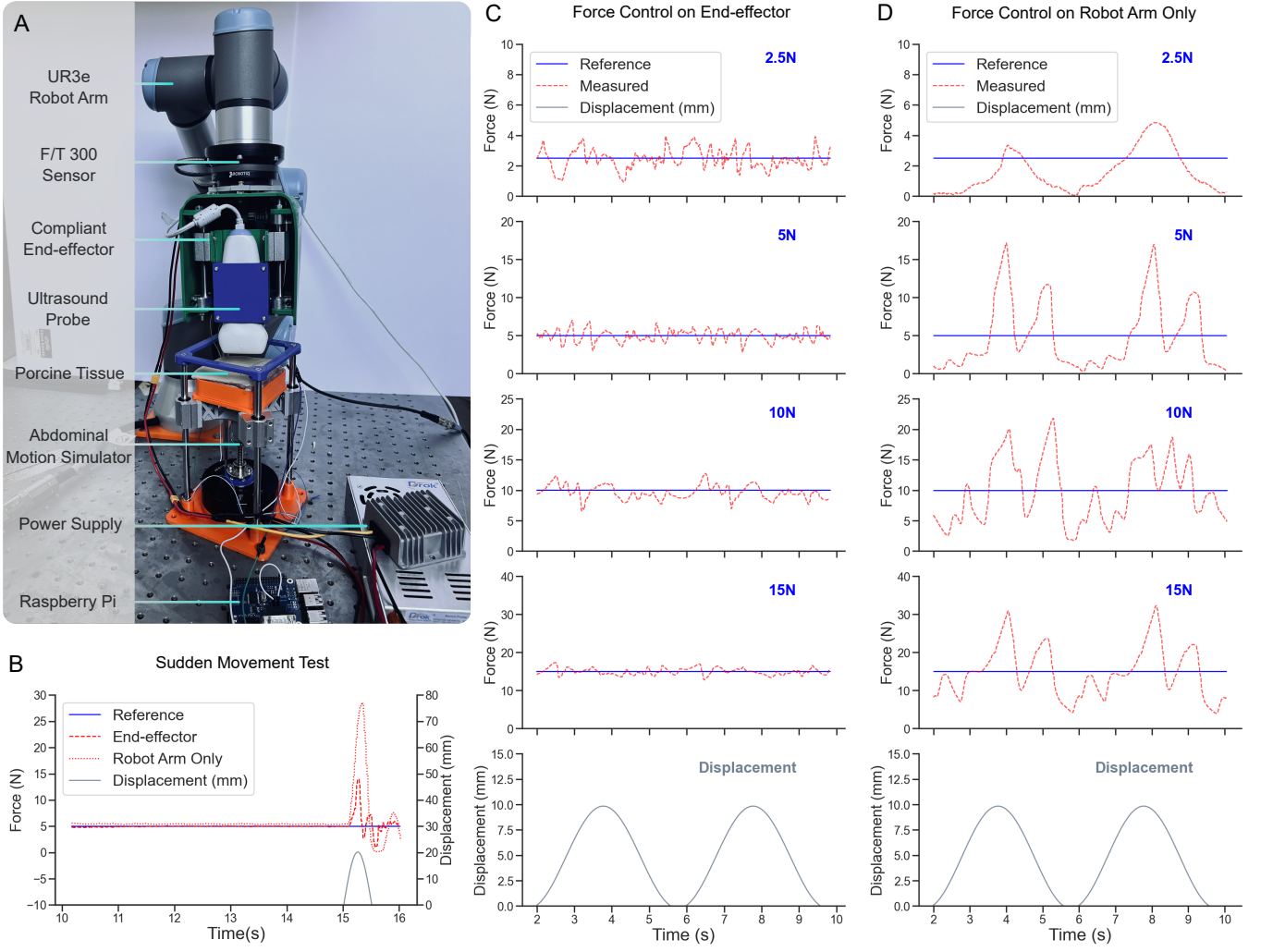


Fig. 2: Experiment setup and force tracking results on porcine tissue with dynamic movement. A: experiment setup of the end-effector attached to the UR3e robot arm; B: Force tracking comparison plot between end-effector and robot arm only conditions under sudden movement while targeting 5N; C: Force tracking plots of the end-effector targeting 2.5N, 5N, 10N, and 15N during simulated breathing motion lasting 8 seconds; D: Force tracking plots of the robot arm targeting 2.5N, 5N, 10N, and 15N during simulated breathing motion lasting 8 seconds

For a timing belt system, the relationship between rotational input and linear output is described by:

$$x_{\text{belt}} = r\theta \quad (1)$$

Where x_{belt} is the linear displacement, r is the radius of the pulley, and θ is the angle of rotation.

In contrast, a crank-slider linkage's motion is described by:

$$x_{\text{crank}} = r(1 - \cos \theta) + \sqrt{l^2 - r^2 \sin^2 \theta} \quad (2)$$

Where x_{crank} is the linear displacement, r is the length of the crank, l is the length of the connecting rod, and θ is the angle of rotation.

The linearity of these systems can be compared by examining their derivatives with respect to θ :

$$\frac{dx_{\text{belt}}}{d\theta} = r \quad (\text{constant}) \quad (3)$$

$$\frac{dx_{\text{crank}}}{d\theta} = r \sin \theta + \frac{r^2 \sin \theta \cos \theta}{\sqrt{l^2 - r^2 \sin^2 \theta}} \quad (\text{variable}) \quad (4)$$

As shown, the timing belt system exhibits a constant rate of change of linear displacement with respect to rotation, while the crank-slider linkage's rate of change varies with θ . This allows for a linear relationship between input rotation and output linear motion and simplifies control for the system.

The complete design is illustrated in Fig. 1. The actuator drives a 96.5mm diameter pulley, which is coupled to a linear slide mechanism housing the US probe. The probe has a maximum travel distance of 52mm, sufficient to accommodate abdominal movement even during deep breathing [23]. The system has a theoretical maximum rated force of 62.2N, exceeding clinical requirements in Table I. The housing is fabricated from PLA plastic. Weighing 1.13 kg, the system

is compatible with small robot arms such as the UR3e, which has a maximum payload of 3 kg. When fully retracted, the system measures only 178mm in length, making navigation around the human body easier compared to longer end-effectors.

C. High Bandwidth and Versatile Mechatronics Architecture

The mechatronics system architecture (Fig. 3) supports two host computer configurations: (1) a stationary desktop computer with a CANable USB-CAN adapter (Protofusion, Ellicott City, MD), or (2) a mobile Raspberry Pi 4 with a PiCAN2 hat (Copperhill Technologies, Greenfield, MA). Both configurations utilize CAN bus 2.0 for communication at speeds up to 1 Mbps. A 48V power supply feeds a buck converter, which steps down the voltage to 24V to drive the AK60-6 QDD actuator. Force measurements are obtained using a six-axis F/T 300 force sensor (Robotiq, Lévis, QC, Canada), sampling at 100 Hz. While current implementations use stationary power sources, the Raspberry Pi-based system is designed to be easily adapted for mobile operation by incorporating a battery pack, making this system suitable for remote or resource-constrained environments. The system architecture also powers our abdominal motion simulator. Experiments were conducted on both the desktop computer and Raspberry Pi configurations.

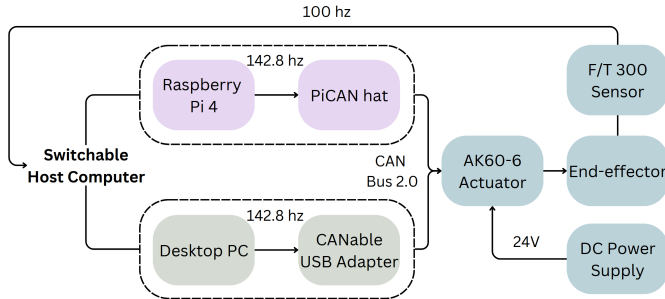


Fig. 3: Mechatronics architecture of the end-effector. The mechatronics setup also powers the *ex vivo* motion simulator.

D. Controller Design

To evaluate the efficacy of the end-effector compared to a robot arm only, we implemented a Proportional-Integral-Derivative (PID) controller, a widely adopted approach that does not necessitate prior model knowledge. The PID controller was applied with positive gain parameters for force control. This approach contributes to stability by not introducing additional energy into the system and maintaining stability through feedback [24]. We implemented the force controller on both the end-effector and the robot arm (Fig. 4). The robot arm’s PID force controller implementation was based on the controller from a previous work [25]. To optimize PID controller performance, we first used the Ziegler-Nichols tuning method as a starting point, then heuristically based on feedback. The gains were tuned until the best performance was observed for each condition. The gains used in the experiments are shown in Table II.

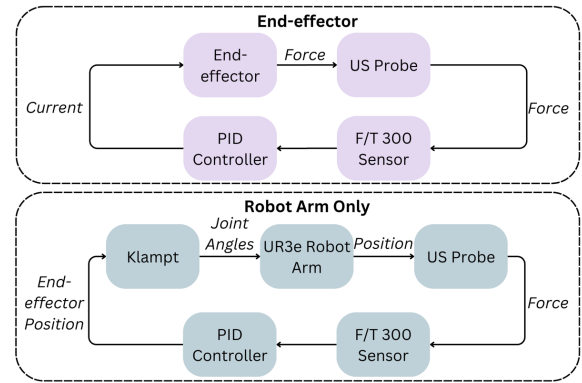


Fig. 4: Controller architecture for both the end-effector and the robot arm. Only one controller is active during their respective experiments. The end-effector uses current-based force control, while the robot arm uses position-based force control.

TABLE II: PID gain values

Controller	k_p	k_i	k_d
1	0.35	2.39	0.0186
2	0.26	2.39	0.01
3	0.429	2.39	0.0186
4	0.54	12.85	0.015
5	0.54	12.85	0.015
6	1.6	0	0.015
7	0.629	8.85	0.015
8	0.529	12.85	0.015
9	0.429	8.85	0.015
10	0.429	8.85	0.015
11	0.03	5×10^{-8}	0.001
12	0.03	5×10^{-8}	0.001
13	0.03	5×10^{-8}	0.001
14	0.025	5×10^{-8}	0.001
15	0.02	5×10^{-8}	0.001

E. Ex Vivo Abdominal Motion Simulator Design

An actuated *ex vivo* tissue platform was developed to mimic the dynamic movements of a human abdomen during breathing. The simulator has two broad components: a tissue staging platform, and an actuation system to simulate the abdomen’s movement during respiration. The tissue platform is designed to hold both *ex vivo* tissue and tissue phantoms. An AK80-9 actuator (Cubemars, Shenzhen, China) drives a lead screw, actuating the tissue platform to move in an axial direction, following a similar approach developed in previous work [26]. The simulator is shown in Fig. 2A. During testing, the platform oscillates in a sinusoidal pattern with an amplitude of 9.9 mm and a frequency of 14.6 cycles per minute, simulating human abdominal movements characteristic of quiet breathing in a supine position [23].

To perform realistic experiments on the proposed end-effector, two sets of tests were done, first on tissue phantom, followed by *ex vivo* porcine abdominal wall tissue, comprising skin, subcutaneous fat, and underlying muscle layers, purchased from a local supermarket. This allowed us to test the end-effector on both homogeneous tissue phantoms and heterogeneous tissue specimens similar to human abdomen tissue. For tissue phantom creation, 2.5%

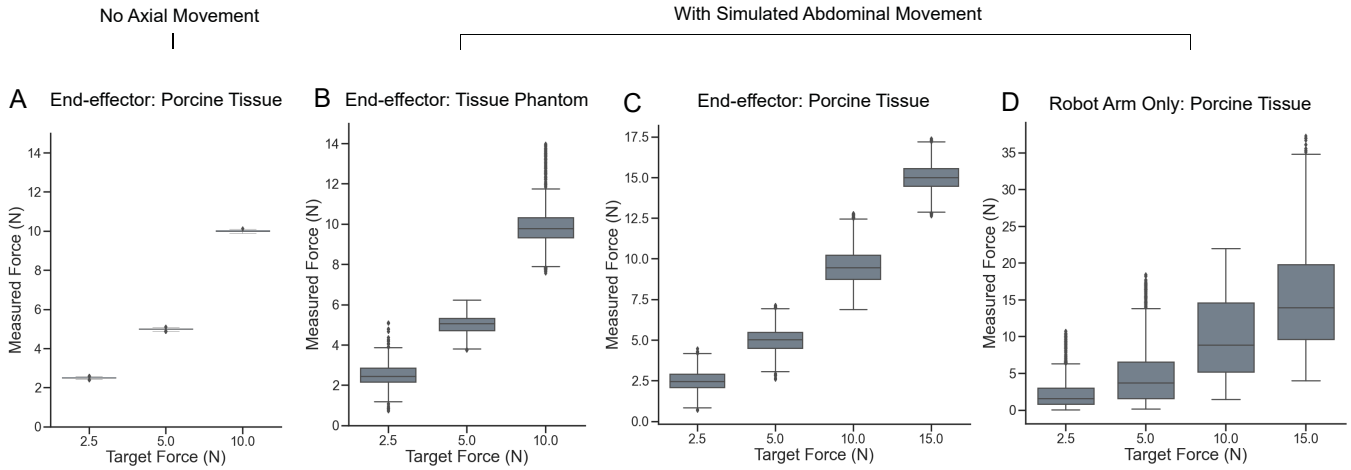


Fig. 5: Force tracking distribution box plots, showing concatenated data from three 8-second measurements (total of 24 seconds) at each target force. A: no motion, end-effector on porcine tissue; B: simulated motion, end-effector on tissue phantom; C: simulated motion, end-effector on porcine tissue; D: simulated motion, robot arm on porcine tissue.

high-acyl gellan gum (% mass) (VWR, P.A., United States) was used following the procedure previously proposed [27]. The developed phantom has Young’s modulus greater than 25 kPa, extrapolating values presented in [27].

III. EXPERIMENTS AND RESULTS

We conducted a series of force tracking experiments to evaluate the performance of our compliant end-effector compared to a UR3e robot arm (Universal Robots, Odense, Denmark). The experiment setup is shown in Fig. 2A. Experiments were performed on porcine abdominal tissue and a tissue phantom under stable and dynamic conditions, simulating respiratory motion and sudden movements. During the end-effector conditions, the robot arm is not powered on. During the robot arm only conditions, the compliant end-effector is replaced with a rigid one. Force measurements were obtained using a six-axis F/T 300 force sensor. Data collection involved recording force measurements at various target forces (2.5N, 5N, 10N, and 15N) over 8-second intervals (two complete cycles of movement), $n=3$ measurements were obtained for each condition except for the sudden movement test which had $n=1$. Mean values and Root Mean Square Error (RMSe) was calculated to assess force tracking accuracy.

A. Force Tracking on End-effector with Porcine Tissue (No Axial Motion)

Force tracking on the end-effector was conducted on porcine tissue at target forces of 2.5N, 5N, and 10N in a stable configuration, without axial motion. The tuned PID values were controllers 1, 2, and 3 respectively in Table II. The system exhibited high precision in maintaining the desired force levels, with mean values of 2.50N (RMSe: 0.03N), 4.99N (RMSe: 0.04N), and 10.00N (RMSe: 0.04N), closely matching the target forces. These results confirm the system’s ability to achieve excellent force tracking under stable conditions. Refer to Fig. 5A for the distribution.

B. Force Tracking on End-effector with Tissue Phantom (Simulated Breathing Motion)

In a dynamic scenario simulating respiratory motion on the abdominal motion simulator (9.9mm displacement, 14.6 breaths per minute [23]), with a tissue phantom and the same target forces. The tuned PID values were controllers 4, 5, and 6 respectively in Table II. The results showed measured mean forces of 2.50N (RMSe: 0.59N), 5.02N (RMSe: 0.46N), and 10.00N (RMSe: 1.12N). These results demonstrated the system’s robustness in adjusting to continuous axial motion, though with slight variations in higher force levels due to the dynamic nature of the experiment, and demonstrate that the end-effector maintained force control effectively on a homogeneous tissue phantom. Refer to Fig. 5B for the distribution.

C. Force Tracking on End-effector with Porcine Tissue (Simulated Breathing Motion)

The same simulated breathing conditions was tested using porcine tissue with target forces of 2.5N, 5N, 10N, and 15N. The tuned PID values were controllers 7, 8, 9, and 10 respectively in Table II. The measured mean forces were 2.50N (RMSe: 0.61N), 5.01N (RMSe: 0.77N), 9.56N (RMSe: 1.09N), and 14.99N (RMSe: 0.86N). These results demonstrate the system obtained comparable results on a more realistic heterogeneous tissue specimen similar to human abdomen tissue, even under high force loads. See Fig. 2C for the force tracking plots, and Fig. 5C for the distribution.

D. Force Tracking on UR3e Robot Arm Only with Porcine Tissue (Simulated Breathing Motion)

The UR3e robot arm, without the compliant end-effector, was tested under the same simulated breathing conditions using a PID controller at 2.5N, 5N, 10N, and 15N. The tuned PID values were controllers 11, 12, 13, and 14 respectively in Table II. The measured mean forces were 2.20N (RMSe: 2.09N), 4.94N (RMSe: 4.30N), 9.97N (RMSe: 5.43N), and

14.96N (RMSe: 6.99N) for the target forces respectively. This increased error reflects the challenges of maintaining precise force control using conventional force control on the robot arm alone, especially in dynamic scenarios. See Fig. 2D for the force tracking plots and Fig. 5D for the distribution.

E. Force Tracking Comparison: UR3e Robot Arm and End-effector with Porcine Tissue (Sudden Movement)

Finally, force tracking was assessed in the event of a sudden 20mm sinusoidal displacement over 0.25s rise time and 0.25s fall time, both the UR3e robot arm and the compliant end-effector were tasked with maintaining a 5N contact force on porcine tissue. The tuned PID values were controller 15 for the robot arm and 2 for the end-effector in Table II. The end-effector demonstrated superior recovery and less maximum force, with contact forces ranging from 0.96N to 13.94N, while the UR3e arm exhibited more pronounced fluctuations, with contact forces ranging from 0.12N to 28.57N. These results show the end-effector's superior ability to maintain stable contact while not applying excessive force under abrupt motion. See Fig. 2B for the comparative tracking plot.

IV. DISCUSSION

A 2024 study revealed that between 2011 and 2021, the growth in ultrasound examinations (55.1%) exceeded the rise in the number of sonographers (43.6%) [2]. The U.S. Bureau of Labor Statistics projects a need for an additional 27,600 sonographers by 2024 [28]. In the UK, recent NHS data shows as of December 2023, about 416,900 patients were waiting 6 weeks or more for key diagnostic tests, including ultrasounds, with one-third of patients waiting more than 6 weeks for diagnostic tests require non-obstetric ultrasounds [29]. Safe and reliable robotic US systems could significantly alleviate this pressure.

The design and validation of the compliant QDD end-effector presented in this paper addresses important compliance challenges in robotic US imaging, primarily focusing on ensuring patient safety through passive mechanical compliance while maintaining precise force control. The experiments demonstrate the efficacy of this design in achieving stable and consistent force application across varying dynamic conditions, particularly in mimicking respiratory motion, which is essential for abdominal imaging. Importantly, it demonstrates much superior force tracking accuracy during dynamic motion and the ability to handle sudden movements compared to a conventional robot arm only system that relies on active compliance force control. Experiments with no axial motion showed an average force tracking error of 0.04N RMSe across 2.5N-10N. Experiments conducted during dynamic movement show that the end-effector has an average force tracking error of 0.83N RMSe across 2.5N-15N, which is much lower than 4.70N RMSe using conventional active compliance force control on only the robot arm, or the 2.47N of variability for manual scans [30]. Compared to soft fluidic end-effectors [12], this work

offers position feedback, achieves higher forces, and regulates force independently of the robot arm. In contrast to pneumatic end-effectors [5], it provides position feedback, reaches both higher and lower forces, and outperforms in static force regulation. Comparisons under dynamic conditions are challenging, as this is the only work, to the authors' knowledge, that incorporates a dynamically moving tissue platform for ultrasound compliance testing.

One limitation of the current system is the use of PLA plastic in constructing the end-effector, which restricted the maximum force to 15N—below the clinical requirement of 17.3N and the actuator's theoretical limit of 62.2N. Forces above 15N caused the PLA structure to deform, leading to inconsistent tension and belt slipping. Future iterations will address this by using tougher materials like carbon-fiber-reinforced nylon or aluminum. Despite this, the end-effector outperforms most compliant robotic US end-effectors, which typically don't exceed 10N. Additionally, the experimental setup, limited to single-axis movement due to the abdominal motion simulator's restricted working area, does not fully replicate real-world multi-axis US scanning. Future work will expand the simulator to enable trajectory scanning across a larger surface area, offering a more comprehensive assessment of the end-effector's capabilities and exploring a safe scanning velocity. This is important because most current systems must operate at slower speeds to maintain safety due to their limited force control bandwidth.

From a clinical perspective, the end-effector's ability to maintain accurate force tracking during dynamic movement is significantly better than using conventional active compliance control on only the robot arm. The precise force tracking could lead to more consistent ultrasound images, enhancing diagnostic accuracy and reducing the need for repeat scans. Additionally, the end-effector's rapid response to sudden movements (peak force of 13.94N compared to 28.57N for the robot arm) suggests a reduced risk of patient discomfort or injury during unexpected patient movements, particularly important in pediatric or geriatric care where compliance may be important.

V. CONCLUSION

This study introduces a novel compliant QDD end-effector for robotic ultrasound imaging, demonstrating improved force control and safety compared to conventional systems. Its superior performance in dynamic scenarios and ability to manage sudden movements make it well-suited for clinical applications and represent a significant step toward safer, more reliable robotic ultrasound systems. Future research will focus on overcoming current limitations and scaling the system for broader clinical applications, such as automated diagnostic imaging in remote or underserved communities.

ACKNOWLEDGMENTS

The authors would like to thank George Delagrammatikas, Brian Mann, Ethan LoCiero, Amy Strong, Kento Yamamoto, and Chad Miller for providing valuable feedback, as well as the Duke Innovation Colab for partially funding this project.

REFERENCES

- [1] D. Fischerova, "Ultrasound scanning of the pelvis and abdomen for staging of gynecological tumors: a review," *Ultrasound in Obstetrics & Gynecology*, vol. 38, no. 3, pp. 246–266, 2011, eprint: <https://onlinelibrary.wiley.com/doi/pdf/10.1002/uog.10054>. [Online]. Available: <https://onlinelibrary.wiley.com/doi/abs/10.1002/uog.10054>
- [2] D. Won, J. Walker, R. Horowitz, S. Bharadwaj, E. Carlton, and H. Gabriel, "Sound the alarm: The sonographer shortage is echoing across healthcare," *Journal of Ultrasound in Medicine*, 2024.
- [3] R. O. Nathan, J. O. Swanson, D. L. Swanson, E. M. McClure, V. L. Bolamba, A. Lokangaka, I. S. Pineda, L. Figueroa, W. López-Gomez, A. Garces, D. Muyodi, F. Esamai, N. Kanaiza, W. Mirza, F. Naqvi, S. Saleem, M. Mwenechanya, M. Chiwila, D. Hamsumonde, D. D. Wallace, H. Franklin, and R. L. Goldenberg, "Evaluation of Focused Obstetric Ultrasound Examinations by Health Care Personnel in the Democratic Republic of Congo, Guatemala, Kenya, Pakistan, and Zambia," *Current Problems in Diagnostic Radiology*, vol. 46, no. 3, pp. 210–215, 2017. [Online]. Available: <https://www.ncbi.nlm.nih.gov/pmc/articles/PMC5413583/>
- [4] K. Li, Y. Xu, and M. Q.-H. Meng, "An Overview of Systems and Techniques for Autonomous Robotic Ultrasound Acquisitions," *IEEE Transactions on Medical Robotics and Bionics*, vol. 3, no. 2, pp. 510–524, May 2021. [Online]. Available: <https://ieeexplore.ieee.org/document/9399640/>
- [5] W.-Y. Kuo, X. Ma, D. Deshmukh, and H. K. Zhang, "Automatic Contact Force-regulated End-effector Using Pneumatic Actuator for Safe Robotic Ultrasound Imaging," in *2023 International Symposium on Medical Robotics (ISMR)*, Apr. 2023, pp. 1–6, iISSN: 2771-9049. [Online]. Available: <https://ieeexplore.ieee.org/document/10130200/>
- [6] Y. Wang, T. Liu, X. Hu, K. Yang, Y. Zhu, and H. Jin, "Compliant Joint Based Robotic Ultrasound Scanning System for Imaging Human Spine," *IEEE Robotics and Automation Letters*, vol. 8, no. 9, pp. 5966–5973, Sep. 2023, conference Name: IEEE Robotics and Automation Letters. [Online]. Available: <https://ieeexplore.ieee.org/document/10198531/?arnumber=10198531>
- [7] S. Virga, O. Zettinig, M. Esposito, K. Pfister, B. Frisch, T. Neff, N. Navab, and C. Hennersperger, "Automatic force-compliant robotic ultrasound screening of abdominal aortic aneurysms," in *2016 IEEE/RSJ International Conference on Intelligent Robots and Systems (IROS)*, Oct. 2016, pp. 508–513, iISSN: 2153-0866. [Online]. Available: <https://ieeexplore.ieee.org/document/7759101/?arnumber=7759101>
- [8] W. Wang, R. N. Loh, and E. Y. Gu, "Passive compliance versus active compliance in robot-based automated assembly systems," *Industrial Robot: An International Journal*, vol. 25, no. 1, pp. 48–57, Jan. 1998, publisher: MCB UP Ltd. [Online]. Available: <https://doi.org/10.1108/01439919810196964>
- [9] K. Mathiassen, J. E. Fjellin, K. Glette, P. K. Hol, and O. J. Elle, "An Ultrasound Robotic System Using the Commercial Robot UR5," *Frontiers in Robotics and AI*, vol. 3, Feb. 2016, publisher: Frontiers. [Online]. Available: <https://www.frontiersin.org/journals/robotics-and-ai/articles/10.3389/frobt.2016.00001/full>
- [10] T.-Y. Fang, H. K. Zhang, R. Finocchi, R. H. Taylor, and E. M. Boctor, "Force-assisted ultrasound imaging system through dual force sensing and admittance robot control," *International Journal of Computer Assisted Radiology and Surgery*, vol. 12, no. 6, pp. 983–991, Jun. 2017.
- [11] M. Chignoli, D. Kim, E. Stanger-Jones, and S. Kim, "The MIT Humanoid Robot: Design, Motion Planning, and Control For Acrobatic Behaviors," Apr. 2021, arXiv:2104.09025 [cs]. [Online]. Available: <http://arxiv.org/abs/2104.09025>
- [12] L. Lindenroth, A. Soor, J. Hutchinson, A. Shafi, J. Back, K. Rhode, and H. Liu, "Design of a soft, parallel end-effector applied to robot-guided ultrasound interventions," Sep. 2017, pp. 3716–3721.
- [13] G. Zoller, V. Wall, and O. Brock, "Acoustic Sensing for Soft Pneumatic Actuators," *2018 IEEE/RSJ International Conference on Intelligent Robots and Systems (IROS)*, pp. 6986–6991, Oct. 2018, conference Name: 2018 IEEE/RSJ International Conference on Intelligent Robots and Systems (IROS) ISBN: 9781538680940 Place: Madrid Publisher: IEEE. [Online]. Available: <https://ieeexplore.ieee.org/document/8594396/>
- [14] H. Das, D. Pool, and E.-J. V. Kampen, "Incremental Nonlinear Dynamic Inversion Control of Long-Stroke Pneumatic Actuators," *2021 European Control Conference (ECC)*, pp. 978–983, Jun. 2021, conference Name: 2021 European Control Conference (ECC) ISBN: 9789463842365 Place: Delft, Netherlands Publisher: IEEE. [Online]. Available: <https://ieeexplore.ieee.org/document/9654927/>
- [15] A. Kakogawa, Y. Mori, T. Fukasawa, N. Kurimoto, S. Tokunaga, T. Tokuda, A. Yamamoto, and S. Kawamura, "A Highly Backdrivable Robotic Arm using Low Friction and High Accuracy Cycloidal Geared Motors: ALFHA," *2022 IEEE/SICE International Symposium on System Integration (SII)*, pp. 428–433, Jan. 2022, conference Name: 2022 IEEE/SICE International Symposium on System Integration (SII) ISBN: 9781665445405 Place: Narvik, Norway Publisher: IEEE. [Online]. Available: <https://ieeexplore.ieee.org/document/9708868/>
- [16] A. Singh, N. Kashiri, and N. Tsagarakis, "Design of a Quasi-Direct-Drive Actuator for Dynamic Motions," *Proceedings*, vol. 64, no. 1, p. 11, 2020, number: 1 Publisher: Multidisciplinary Digital Publishing Institute. [Online]. Available: <https://www.mdpi.com/2504-3900/64/1/11>
- [17] M. Dhyani, M. Gilbertson, A. Anvari, B. Anthony, and A. Samir, "Precise quantification of sonographic forces: a first step toward reducing ergonomic injury," *American Institute of Ultrasound Medicine (Las Vegas, NV)*, 2014.
- [18] C. A. Pérez-Díaz, I. Muñoz, D. Martín-Hernández, C. Candelo-Zuluaga, I. Torres, J. Marsà, D. Sanz-Merodio, and M. López, "Design and experimental characterisation of a novel quasi-direct drive actuator for highly dynamic robotic applications," in *2024 IEEE International Conference on Robotics and Automation (ICRA)*, 2024, pp. 183–189.
- [19] M. Li, A. Pal, A. Aghakhani, A. Pena-Francesch, and M. Sitti, "Soft actuators for real-world applications," *Nature Reviews Materials*, vol. 7, no. 3, pp. 235–249, 2022.
- [20] B. Katz, J. D. Carlo, and S. Kim, "Mini cheetah: A platform for pushing the limits of dynamic quadruped control," in *2019 International Conference on Robotics and Automation (ICRA)*, 2019, pp. 6295–6301.
- [21] A. Azocar, L. Mooney, J.-F. Duval, A. Simon, L. Hargrove, and E. Rouse, "Design and clinical implementation of an open-source bionic leg," *Nature Biomedical Engineering*, vol. 4, pp. 1–13, Oct. 2020.
- [22] Y. Long and Y. Peng, "Design and Control of a Quasi-direct Drive Actuated Knee Exoskeleton," *Journal of Bionic Engineering*, vol. 19, no. 3, pp. 678–687, May 2022. [Online]. Available: <https://doi.org/10.1007/s42235-022-00168-2>
- [23] H. Kaneko and J. Horie, "Breathing movements of the chest and abdominal wall in healthy subjects," *Respiratory care*, vol. 57, no. 9, pp. 1442–1451, 2012.
- [24] D. Zonetti, G. Bergna-Díaz, R. Ortega, and N. Monshizadeh, "Pid passivity-based droop control of power converters: Large-signal stability, robustness and performance," *International Journal of Robust and Nonlinear Control*, vol. 32, no. 3, pp. 1769–1795, 2022.
- [25] S. Rigby Oca, A. Strong, J. Havas, D. M. Buckland, and L. J. Bridgeman, "Development and testing of a durable and novel breast phantom for robotic autonomous ultrasound systems," *Journal of Medical Robotics Research*, vol. 7, no. 04, p. 2241010, 2022.
- [26] D. Chen, C. Krinsky, M. Phillips, C. Allred, A. Khan, L. B. Liu, U. Christians, and S. K. Yazdani, "Design and use of an ex vivo peripheral simulating bioreactor system for pharmacokinetic analysis of a drug coated stent," *Bioengineering & Translational Medicine*, vol. 9, no. 2, p. e10618, 2024, eprint: <https://onlinelibrary.wiley.com/doi/pdf/10.1002/btm2.10618>. [Online]. Available: <https://onlinelibrary.wiley.com/doi/abs/10.1002/btm2.10618>
- [27] R. Prakash, K. K. Yamamoto, S. R. Oca, W. Ross, and P. J. Codd, "Brain-mimicking phantom for photoablation and visualization," in *2023 International Symposium on Medical Robotics (ISMR)*. IEEE, 2023, pp. 1–7.
- [28] "Current Issues and Opportunities in Sonography | GE Healthcare (United States)." [Online]. Available: <https://www.gehealthcare.com/insights/article/current-issues-and-opportunities-in-sonography>
- [29] "SoR urges workplace reform in response to NHS waiting list numbers." [Online]. Available: <https://www.sor.org/news/government-nhs/sor-urges-workplace-reform-in-response-to-nhs-wait>
- [30] R. Tsumura and H. Iwata, "Robotic fetal ultrasonography platform with a passive scan mechanism," *International Journal of Computer Assisted Radiology and Surgery*, vol. 15, no. 8, pp. 1323–1333, Aug. 2020. [Online]. Available: <https://doi.org/10.1007/s11548-020-02130-1>